Tunneling states in strained alkali-halide crystals containing CN^- ions

Karen A. Topp* and R. O. Pohl†
Laboratory of Atomic and Solid State Physics, Cornell University, Ithaca, New York 14853-2501
(Received 15 March 2002; revised manuscript received 14 May 2002; published 13 August 2002)

Torsional oscillators (~90 kHz) have been used between 0.06 and 100 K to study low-energy excitations in strained alkali-halide hosts doped with KCN in the concentration range from 0.2 to 5 mol %. The tunneling model, originally developed to describe the low-temperature thermal and elastic anomalies in amorphous solids, has been found to describe our data very well. From the observation that the tunneling strength varies linearly with the KCN concentration, we conclude that random internal stresses in the hosts, rather than interactions between the dopant ions, lead to the tunneling states. Implications for the origin of the tunneling states in amorphous solids and in highly disordered crystals, and also for their universality are considered.

DOI: 10.1103/PhysRevB.66.064204 PACS number(s): 63.50.+x, 65.60.+a

I. INTRODUCTION

The vibrational anomalies observed in amorphous solids at low temperatures[1] have been successfully described with the tunneling model.[2,3] This model assumes that a certain number of atoms or groups of atoms can move between nearly equal potential minima by a tunneling process. Random strains lead to some inequality of the potential minima, and also of the barriers through which the tunneling occurs, and it was argued that these effects might lead to a constant density of tunneling states, or more precisely, of what is now called their spectral density $\overline{P}$.[4] With the assumption that all tunneling states in a given solid have the same coupling energy, γ, to the lattice strains, a quantity C, now called tunneling strength, is defined

$$C=\frac{\overline{P}\gamma^2}{\rho v^2}, \tag{1}$$

where ρ is the mass density, and v is the speed of sound of the solid (subscripts signifying the polarization of the waves, l and t, have been omitted for simplicity). C, together with $\overline{P}$ and γ, have been used to describe the vibrational anomalies[5–8] observed in these solids.

This model treats the tunneling defects as isolated and noninteracting, and it also makes no attempt to explain the remarkable observation that in all amorphous solids the tunneling strength was found to have approximately the same magnitude, within an order of magnitude, regardless of chemical composition. This fact appears by now to be well established experimentally, with very few exceptions.[4,9] In order to explain this universality it was suggested[10] that the tunneling defects, which distort the lattice, interact with each other, and will lead to a density of states of the tunneling defects given by

$$n(E)=\frac{\rho v^2}{\gamma^2}. \tag{2}$$

Since $n(E)$ is approximately ten times larger than $\overline{P}$ [for details, see below, Eq. (9)] it follows from Eq. (2) that

$$C=\frac{\overline{P}\gamma^2}{\rho v^2}=0.1. \tag{3}$$

However, this value is between two and three orders-of-magnitude larger than the one found experimentally ($10^{-4}<C<10^{-3}$).[9] In an attempt to remove this discrepancy, it was therefore suggested[11] that additional elastic dipoles might exist in the amorphous structure which do not tunnel, but which will lead to a limitation of the tunneling state density. Parshin[11] argued that by including oscillators vibrating in quasiharmonic potentials as postulated in the soft potential model, Eq. (3) could be satisfied, and the universality explained. For the purpose of the present investigation, it suffices to say that an expression of the form of Eq. (1) appears in the description of the tunneling states, regardless of whether or not interaction between the defects is considered. This similarity raises the fundamental question as to the role interactions play in the physical origin of the tunneling states in amorphous solids.

In the present investigation, we will try to answer experimentally the question of whether random stresses by themselves, without any interactions between the defects (a basic assumption of the tunneling model), can lead to the constant spectral density $\overline{P}$. In order to do this, we will use crystals as hosts for molecular tunneling impurities. As the tunneling defects, we choose CN^- ions. In many alkali-halide host lattices, such as KCl or KBr, these ions form tunneling states as the dumbbell-shaped CN^- moves between eight equilibrium orientations in the [111] directions on the lattice site.[12,13] These states have been studied extensively, for example, through specific-heat measurements, where they are observed through a Schottky anomaly, or through thermal conductivity, where they cause phonon resonant scattering, as reviewed in Ref. 14. Interactions between the CN^- ions in the KBr host have also been observed in recent work at concentrations as small as 1000 ppm,[15] or possibly even at 340 ppm.[16,17]

It has been reported by Watson that the addition of CN^- into the mixed host crystal $(KBr)_{0.5}(KCl)_{0.5}$ leads to entirely new effects even at small concentrations.[18] Instead of a narrowly peaked Schottky anomaly, a specific-heat anomaly varying linearly with temperature was observed, and the

thermal conductivity did not show a resonance ''dip,'' but varied as the temperature squared. Watson showed that these together with some acoustic observations could be well described with the tunneling model. A similar conclusion was also reached by Enss *et al.* in a study of the rotary echo signal in $(RbBr)_{0.5}(KBr)_{0.5}$ containing 70 ppm CN^-.[19] Watson suggested that random strains resulting from the random mixing of the large Br^- ions with the smaller Cl^- ions were leading to the glasslike behavior. The work to be reported here follows from this investigation. We will study, in three differently strained host lattices, the effect of CN^- ions as a function of concentration. We will concentrate on elastic measurements, which have been found to be particularly sensitive to the predictions of the tunneling model. In the analysis, however, we will include the earlier measurements by Watson, including the thermal ones. Overall, we will vary the CN^- concentration from 0.2 mol % to 5 mol %, well into the range in which interactions dominate all effects in unstrained host lattices,[20] and will explore how the tunneling strength varies with the CN^- concentration.

The obvious question which must be addressed is what, if anything, can be learned about amorphous solids from studying a doped crystal. Two answers can be given: (i) Molecular dopants (e.g., NO_2^-) have been introduced into amorphous solids (e.g., B_2O_3) in an attempt to modify the tunneling strength of C (reviewed in Ref. 9). No changes were achieved, which is, of course, just another piece of evidence for the universality of C. Thus, the use of any dopants in amorphous hosts is not a promising avenue for the study of the effect of strains. (ii) The vibrational anomalies first observed in amorphous solids have since been observed in a wide range of chemically disordered crystalline solids, and have also been shown to be absent in some (very few) amorphous ones, as also reviewed in Ref. 9. The conclusion drawn from these observations is that the amorphous structure, by itself, is not the cause for the anomalies. Their origin might therefore as well be studied in crystalline matrices.

II. EXPERIMENTAL DETAILS

A. Sample preparation

All of the CN^--doped crystals investigated here, KBr, KCl, and the mixed crystals KBr_{1-x} KCl_x, and $RbCl_{1-x}$ KCl_x have the sodium chloride crystal structure in which the elongated CN^- ion substitutes for a halide ion, as illustrated in Fig. 1. It is possible to grow single crystals of CN^--doped single host alkali halides over the full range of composition.[21] In the mixed host $(KBr)_{1-x}(KCl)_x$, however, which is strained due to the random mixing of disparate ion sizes and lattice constants (see Table I), we have found that when adding over 4% or 5% KCN to this mixture, it became difficult to pull a crystal from the melt (the crystal tends to pinch off, not wanting to add lattice planes to the starting seed crystal), and so our mixed host data are limited to a 5% CN^--dopant concentration. Interestingly, we found that once a strained host crystal is grown, the CN^- seems to act like ''glue'' in keeping it together; $(KBr)_{.5}(KCl)_{.5}$ with no CN^- shatters readily, whereas increasing amounts of cyanide make the crystals more and more difficult to cleave.

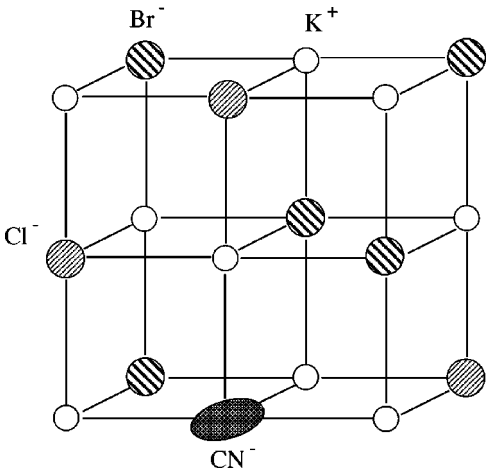

FIG. 1. Sodium chloride structure of $(KCl)_{1-x}(KBr)_x$ mixed crystals doped with CN^-. The random substitution of Br^- for Cl^- leads to a disordered crystal with no glasslike excitations detected in thermal-conductivity experiments (Refs. 53 and 18). For $(KCl)_{1-x}(RbCl)_x$, which has the same structure, only thermal-conductivity measurements exist for $x=0.01$, which are, however, indistinguishable from those of $(KCl)_{0.99}(KBr)_{0.01}$ (Ref. 54), thus not giving any indication for glasslike excitations. The CN^- enters the lattice substitutionally.

The crystals measured here were seed pulled from the melt by Gerhard Schmidt in the Crystal Growth Facility of the Cornell Center for Materials Research. The starting powders of KCl, KBr, and RbCl were Merck Industries ''superpure,'' with nominal impurity levels of less than 1 ppm. A check of the OH^- level in our crystal of ''pure'' KCl, via UV absorption ($\lambda=2045$ Å), confirmed a concentration of ~ 0.5 ppm. The cyanide added to these crystals was taken from one of two seed-pulled single crystals of KCN, grown at Cornell and by F. Lüty in the Crystal Growth Laboratory at Utah, for which the starting powder had been vacuum baked to remove H_2O. Even with these precautions, there are still noticeable amounts of NCO^- in our doped crystals [detected by infrared (IR) absorption], present at the level of ~ 600 ppm in the samples doped with several percent KCN, to ~ 5 ppm in the ''pure'' undoped KCl and $(KBr)_{.5}(KCl)_{.5}$ samples. (The latter amount of NCO^- in undoped samples agrees with the amounts found in the ''pure'' samples of Ref. 22.)

The concentrations of CN^- in the crystals used in this study were determined by IR absorption at room temperature. The fundamental stretching vibration of CN^- is ~ 2100 cm^{-1} (wave numbers) for all crystal hosts used; the measured absorption peaks, especially with mixed host crystals, were seen to be quite wide, however, and so the peak absorption value relationships of Seward and Narayanamurti[22] were not used here. Instead, a ''standard'' sample of $(KBr)_{.3}(KCl)_{.7}+3.0\%$ CN^- (in the melt) was measured for us by Lüty where he performed a careful IR scan and integrated the peak area, using the known oscillator strength of CN^- (to find in that crystal the concentration to be 2.5%). Our measured absorption peak areas were compared to this standard to determine CN^- concentration. The

TABLE I. Crystal structure reference values. The lattice constants and densities are taken from Landolt-Börnstein tables (Ref. 45), and the ionic radii from Ref. 46. The value $N=4/a^3$ is the number density of *halide* sites, useful in converting CN^- concentrations between number/cm^3 and mole fraction (or ppm).

Crystal	a (Å)	N (cm^{-3})	ρ (g cm^{-3})	Crystal ion	Ionic radius (Å)
KCl	6.2929	1.61×10^{22}	1.989	Cl^-	1.81
KBr	6.5982	1.39×10^{22}	2.750	Br^-	1.96
KCN	6.59 [a]	1.40×10^{22}	1.60 [b]	K^+	1.33
RbCl	6.5898	1.40×10^{22}	2.803	Rb^+	1.47
$(KBr)_{0.46}(KCl)_{0.54}$	6.434 [c]	1.50×10^{22}	2.365 [d]		

[a]Reference 47.
[b]Reference 20.
[c]Measured, this work.
[d]Mass density based on lattice constant; note that our measured density of 2.42 g cm^{-3} is 2% higher than this.

conversion factor, given below, is based on the peak area in "absorbance" (abs) versus inverse wavelength (λ^{-1}) graphs, where absorbance is defined as $\log_{10}(I_o/I)$ and I_o and I are the IR intensity values before and after passing through the sample:

$$\frac{\text{peak area}}{\text{sample length}} = 108\frac{abs\times\text{cm}^{-1}}{\text{cm}} \hat{=} 1\%\ \ CN^-. \qquad (4)$$

The density of each crystal was determined using Archimedes' principle by weighing each sample suspended in air and in paraffin oil ($\rho=0.835$ g/cm^3). Lattice-constant measurements were performed on an x-ray powder diffractometer (Cu $K\alpha$ beam) to determine the relative amounts of a mixed host crystal, e.g., $(KBr)_{1-x}(KCl)_x$, by interpolating between values for each pure host (Vegard's law[23]). Measured lattice constants were the following ($\pm.001$ Å): 6.294 Å for KCl—note this is 0.02% higher than the published value given in Table I; 6.434 Å for $(KBr)_{0.46}(KCl)_{0.54}$—called $(KBr)_{0.5}(KCl)_{0.5}$ for simplicity in the following; 6.378 Å for $(KBr)_{0.3}(KCl)_{0.7}$; and 6.440 Å for $(RbCl)_{0.5}(KCl)_{0.5}$.

III. TORSIONAL OSCILLATOR MEASUREMENTS AND ANALYSIS

Internal friction and speed of sound were measured in torsion near 90 kHz, using a composite oscillator technique described in detail by Cahill and Van Cleve.[24] The crystal samples were cleaved along ⟨100⟩ planes into rods of approximately 2×2 mm^2 cross section, with lengths on the order of 8 mm, depending on their transverse speed of sound. The sample and quartz transducer were then formed into a composite torsion bar: The cylindrical transducer was first attached to a thin BeCu pedestal with a drop of Stycast 2580FT epoxy (less than 1.0 mg). The sample was then epoxied to the other end of the transducer, after epoxying a $\sim$0.25-mm thick indium foil ($\sim$0.38 mm for the strained mixed crystals) between sample and transducer to cushion the differences in thermal contraction between them. (Even with the indium foil, the temperature of the strained lattice crystals must be changed very slowly, especially above liquid-nitrogen temperature, to avoid cracking.) The sample length was tuned[25] to be one-half of a shear wavelength so that the composite oscillator has a resonance frequency at room temperature within 1% of the measured quartz-transducer resonance; this adjustment ensures that the epoxy and indium joint between the quartz and sample has almost zero strain, and therefore contributes minimally to the observed internal friction. The oscillator was driven by a set of electrodes which form a quadrupole configuration around the transducer and which simultaneously drive and detect its motion. It was mounted in an insertable cryostat[26] for temperatures above 1.5 K, and in a standard dilution refrigerator for temperatures below. All measurements were taken at an angular strain amplitude between 5×10^{-9} and 5×10^{-8} as described by Liu *et al.*[27] and by Thompson[28] to ensure that the oscillators were driven in a strain-amplitude independent range, as demonstrated through a line shape which was accurately Lorentzian.

Calculation of the internal friction of the sample from that of the composite oscillator is given in detail elsewhere. Note that in our analysis, for convenience even the background (e.g., clamping) losses are included in the sample internal friction.[29] We refer to the same publication for a review of the tunneling model used to evaluate the measurements.

IV. EXPERIMENTAL RESULTS

A. Unstrained hosts

The internal friction of KCl depends strongly on temperature and also on the CN^- doping (Fig. 2). The undoped sample shows a narrow peak at 40 K, and a broad shoulder peaking at 0.2 K. When instead a pure quartz or fluorite crystal sample was attached to the quartz transducer, with an indium foil of similar thickness as that used for the KCl sample epoxied in between, no such broad shoulder or peak were seen.[29] We therefore conclude that these are caused by trace impurities. The dash-dotted line indicates our estimate of the low-temperature internal friction background of a perfect, pure KCl sample.

Doping with as little as 45-ppm CN^- completely changes the internal friction of the sample. Two peaks, one at $\sim$0.5, the other at $\sim$1.5 K, increase the damping by as much a

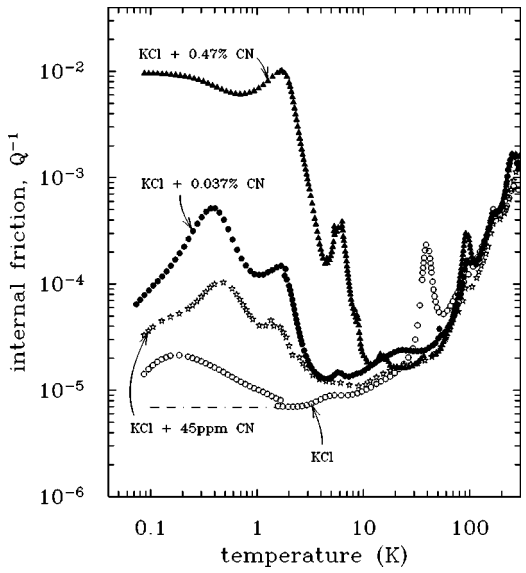

FIG. 2. Internal friction of pure and CN^--doped KCl. Even the undoped crystal shows damping which peaks at 0.2 K, 40 K, and 170 K, believed to be caused by residual impurities. The peaks lie on top of a background internal friction which rises continuously with temperature, most likely due to clamping losses.

factor of 7, while the 40-K peak disappears. When the doping level is increased by another factor of 8, to 375 ppm (0.037%), the two low-temperature peaks increase by a factor of 4 or 5, with a small, but discernible shift in the temperature of the 0.5-K peak. Two new, narrow peaks arise at 6 K and at 90 K. When the CN^- concentration increases by another order of magnitude, to 0.467%, the 1.5-K peak increases by almost two orders of magnitude, while its position shifts to ~ 2 K, while the low-temperature peak disappears under a broad shoulder extending below 0.1 K. The 6-K peak increases drastically, as does the 90-K peak, and another new peak arises at 14 K. The main features observed on the KCl with the highest doping level remain nearly unchanged when the host is changed to KBr,[18,30] as shown in Fig. 3. Thus, the host lattice does not seem to play a significant role.

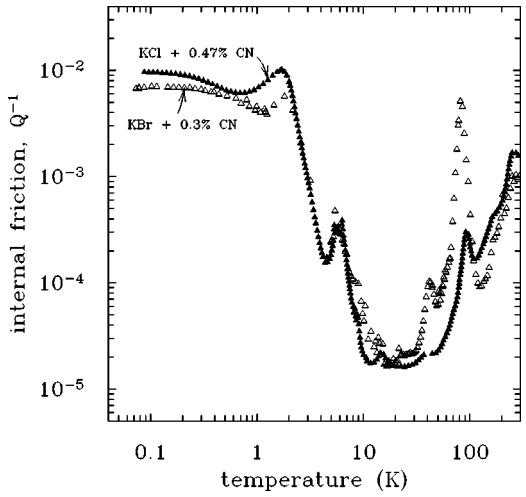

FIG. 3. Internal friction is fairly independent of the host, KCl or KBr, in particular below 10 K.

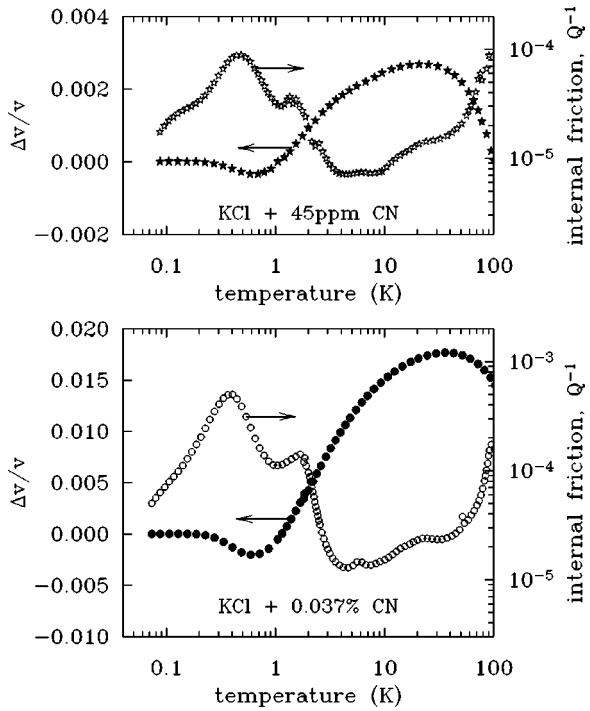

FIG. 4. Comparison of internal friction and change in speed of sound for two CN^- concentrations. Reference velocity, v, for $\Delta v/v$ is measured at the lowest temperature.

As expected, the speed of sound changes together with the internal friction, as shown in Fig. 4 for the two smallest CN^- concentrations, and in Fig. 5 for 0.47% doping in KCl. The extremely large decrease observed in Fig. 5 as the tempera-

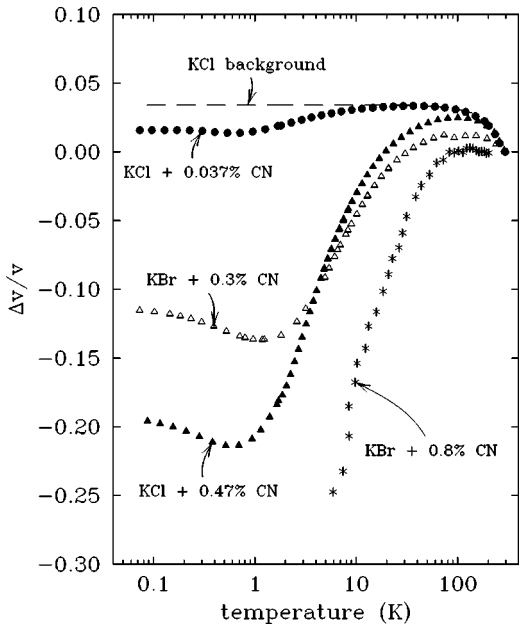

FIG. 5. Drastic lowering of the torsional speed of sound for KCl and KBr containing small CN^- concentrations. KCl, this work; KBr + 0.3% CN (Ref. 30), 80 kHz; KBr + 0.8% CN (Ref. 31), 10 MHz. Reference velocity is measured at 300 K.

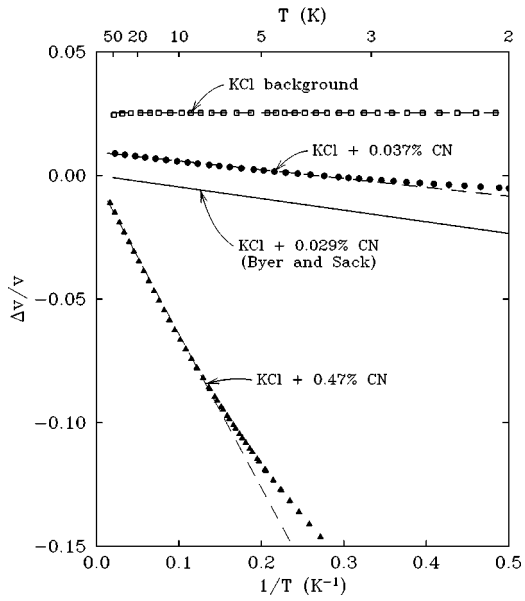

FIG. 6. Same softening in speed of sound as shown in Fig. 5, from 50 K to lower temperatures, but plotted against the inverse temperature. Solid line represents measurements by Byer and Sack (Ref. 32) at 30 MHz.

ture decreases, is also observed in the KBr host for similar doping levels.[30,31] These velocity changes demonstrate a very large softening extending to below 0.1 K.

In one of the first investigations of alkali halides doped with alkali cyanides, Byer and Sack[32] reported a speed of sound in KCl:CN varying proportionally to the inverse temperature, which they explained with the relaxation of classical elastic dipoles. Some of their data are reproduced in Fig. 6, using an inverse temperature scale, together with our own data for KCl containing 0.037% and 0.47% CN^-. Our data

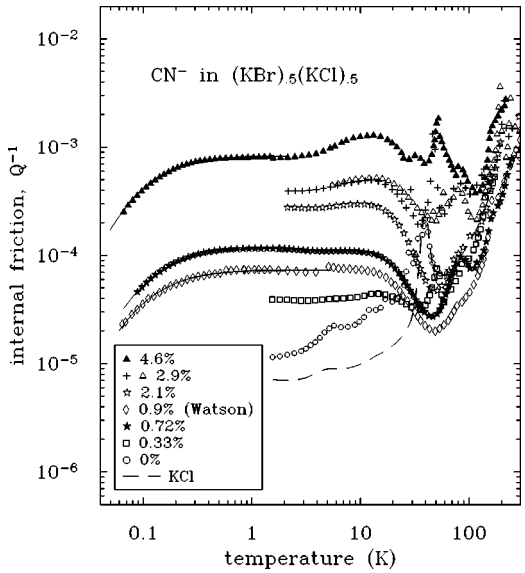

FIG. 7. Internal friction of the mixed crystal system $(KBr)_{0.5}(KCl)_{0.5}$ containing six different CN^- concentrations. The 0.9% data are from Ref. 18. The three solid curves are tunneling model fits, whose parameters are given in Table II below.

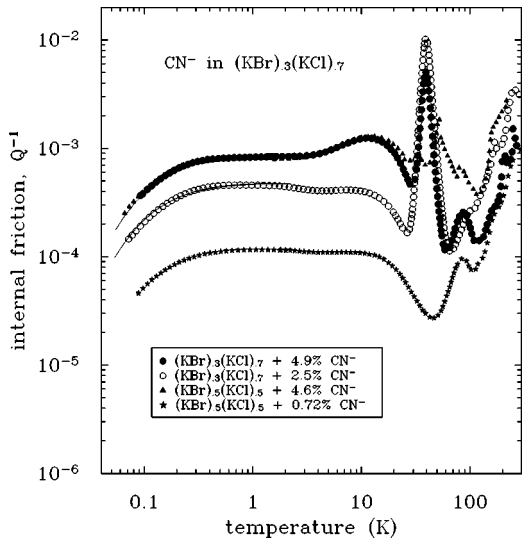

FIG. 8. Internal friction of CN^- in $(KBr)_{0.3}(KCl)_{0.7}$. The solid curves are tunneling model fits; parameters listed in Table II below. For comparsion, two sets of data have been added for doped $(KBr)_{.5}$ $(KCl)_{.5}$. They have been taken from Fig. 7.

also show the T^{-1} dependence reported by Byer and Sack. (The question of whether the slightly smaller slope we observe for the larger concentration—instead of the other way around—is caused by accidental impurities in our samples which have blocked the motion of some of our CN^- ions, or whether the error lies in the determination of the CN^- concentration, must be left open.)

The dynamic response of an isolated [111] quantum impurity has recently been studied by Nalbach *et al.*,[33] and has been applied to these data. They were able to explain the sound velocity for the smallest CN^- doping in KCl, 45 ppm, shown here in Fig. 4, and in particular the peak at 0.5 K observed in internal friction (Fig. 2). However, they could

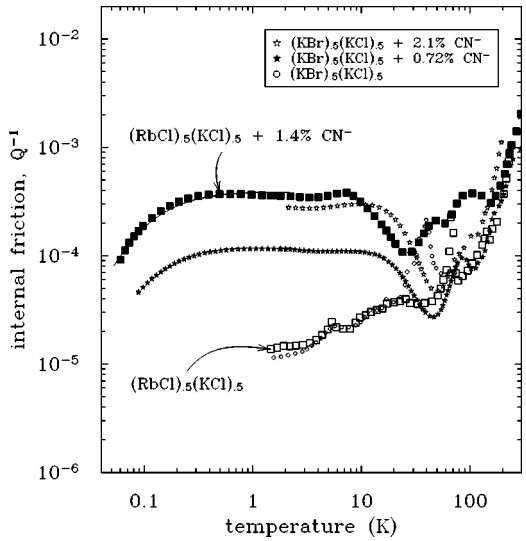

FIG. 9. Internal friction of CN^--doped $(RbCl)_{0.5}(KCl)_{0.5}$ compared to data obtained in doped $(KBr)_{0.5}(KCl)_{0.5}$. Note that the undoped strained hosts have very similar internal friction, showing no sign of a temperature-independent plateau.

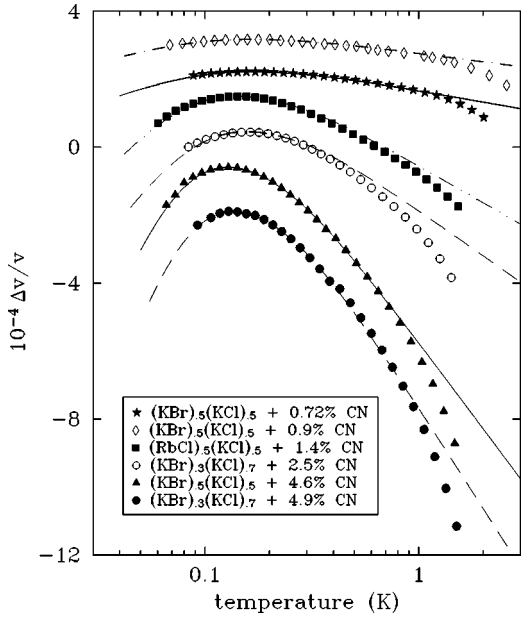

FIG. 10. Speed of sound in all doped mixed hosts in which measurements extended below 1 K. The 0.9% data are taken from Ref. 30.

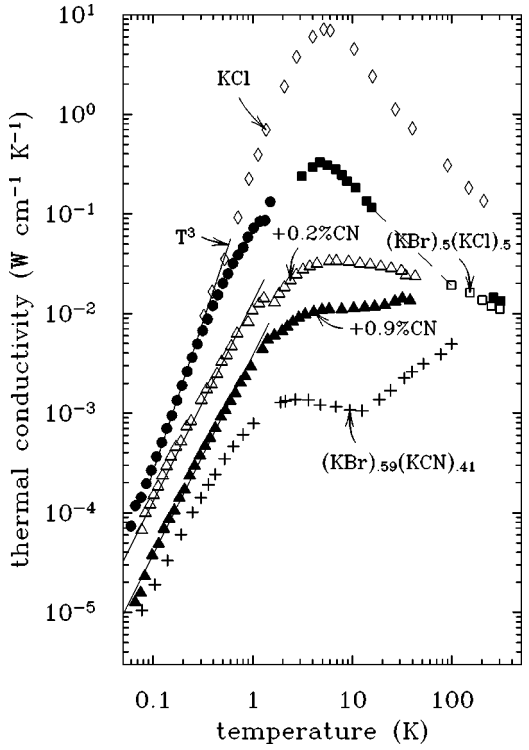

FIG. 11. Thermal conductivity of undoped KCl (diamonds) (Ref. 54) and of $(KBr)_{0.5}(KCl)_{0.5}$ above 1 K (open and filled squares), taken from Ref. 53. Data below 1 K (filled circles) on the mixed crystal from Ref. 18. The solid line through the latter data, below 0.6 K, is the Casimir prediction for boundary scattering for this sample (Ref. 18). Thermal conductivity of $(KBr)_{0.59}(KCN)_{0.41}$ (plus signs) from Ref. 20, with corrected composition according to Ref. 48. Data on the strained host $(KBr)_{0.5}(KCl)_{0.5}$ containing 0.2% and 0.9% CN^- (open and filled triangles, respectively) from Ref. 18. The solid lines through the latter data (below 1 K) are T^2 fits to the data, see Eq. (5).

not explain the second peak of the internal friction at 2 K, and concluded that it might be the first evidence for defect interactions which become increasingly more pronounced as the CN^- concentration increases. To summarize, the acoustic measurements on KCl:CN and KBr:CN demonstrate the remarkable impact of even small cyanide concentrations, but also reveal a rich complexity indicative of defect interactions.

B. Strained hosts

CN^- doping of strained mixed-crystal hosts leads to entirely different and simpler results, at least below ~ 10 K, as shown in Figs. 7–10. The internal friction of the undoped mixed crystals is only somewhat larger in $(KBr)_{0.5}(KCl)_{0.5}$ than in KCl, and is similar to that of $(RbCl)_{0.5}(KCl)_{0.5}$. In these mixed crystals, only few additional relaxation processes seem to exist. Similarly, the speed of sound varies very little with temperature, by less than 10 ppm between 1 K and the lowest temperature of measurement, 0.06 K, and as such has not been shown in Fig. 10.

The addition of CN^- ions completely changes this: The internal friction becomes independent of temperature, until it begins to decrease below ~ 0.5 K, and this plateau value appears to increase linearly with the CN^- concentration. The speed of sound increases noticeably with decreasing temperature, and subsequently decreases below ~ 0.15 K. The observed steepness of $\Delta v/v$ increases with increasing CN^- concentration.

The behavior observed in the doped mixed crystals resembles that observed in amorphous solids, except, of course, the dependence on the amount of doping. We have tested this resemblance by fitting the data to the prediction of the tunneling model. Since the fitting procedure has been described repeatedly in recent publications,[34,35,29] it will not be repeated here. By adjusting the tunneling strength C_t and the coupling energy γ_t, best fits to each of the experimental curves were achieved [the subscript indicates that the measurements were performed with transverse waves]. The fits are shown in Figs. 7 –10 as solid or dashed lines, and they fit the data so well that some of them are difficult to discern from the data. The only significant difference between the prediction of the model and the data is observed for the speeds of sound, Fig. 10, close to and above 1 K, where the data decrease more rapidly than predicted as the temperature increases. However, even this discrepancy is known for amorphous solids, as shown, for example, for a-SiO_2 in Ref. 29. It is concluded that the low-temperature acoustic anomalies observed in the doped strained hosts are fit very well by the tunneling model. The parameters determined from the fits are listed in Table II.

Watson had shown that both the low-temperature thermal conductivity and the specific heat of the doped strained crystals resembled that of amorphous solids. In order to compare the tunneling model parameters obtained from those measurements with those determined from the acoustic measurements, we reproduce Watson's thermal data here. (Note, however, we calculate tunneling model parameters from our

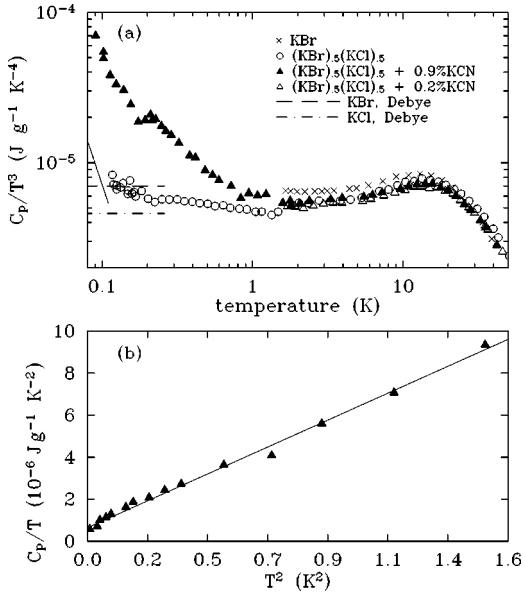

FIG. 12. (a): Specific heat divided by T^3 for $(KBr)_{0.5}(KCl)_{0.5}$, open circles. (The experimental addenda have not been subtracted, but their effect is estimated and shown as a straight line.) Note a $\sim$20% jump at the switch from the dilution cryostat (sample mass, 4.3 g) to an insertable one (sample, 0.27 g). The solid triangles show $(KBr)_{0.5}(KCl)_{0.5}$ containing 0.9% CN^-. Open triangles are 0.2% CN^-, measured above 1.7 K only. All measurements above 1.7 K are from Ref. 30; below, from Ref. 18. Note that the hump occurring at $\sim$15 K in the strained crystal is not changed in the doped crystals. Pure KBr (Ref. 48) is shown here by crosses. The dashed line is pure KBr, measurements from Ref. 20, where $c_D = (70\pm7)\times10^{-7}$ Jg^{-1}K^{-4}, $\theta = 167$ K, $v_D = 1.85$ km/s. The dash-dotted line is pure KCl, after Ref. 14 (see Fig. 28 therein), where $c_D = 46\times10^{-7}$ Jg^{-1}K^{-4}, $\theta = 225$ K, $v_D = 2.37$ km/s; note a numerical error of θ in that figure. (b) Specific heat of the $(KBr)_{0.5}(KCl)_{0.5}$ sample containing 0.9% CN^-, plotted as C_p/T versus T^2. From the intercept we determine $c_1 = 6.4\times10^{-7}$ Jg^{-1}K^{-2}, and from the slope, $c_3 + c_D = (0.2+5.4)\times10^{-6}$ Jg^{-1}K^{-4}. The Debye term, c_D, is obtained from the undoped mixed-crystal value near 2 K. [See (a).] This value of c_D corresponds to $\theta = 195$ K, and $v_D = 2.11$ km/s. In order to avoid misunderstandings, it is emphasized that the value of the ascissa in Fig. 12(b) extends to a maximum value of 10^{-5} J g^{-1}K^{-2}.

own fits of the model to her data.) Figure 11 compares the thermal conductivity of undoped $(KBr)_{0.5}(KCl)_{0.5}$ and that of the 0.2% and 0.9% CN^--doped mixed crystals with that of pure KBr and of the mixed crystal $(KBr)_{0.59}(KCN)_{0.41}$. The latter belongs to the mixed series $(KBr)_{x-1}(KCN)_x$, in which glasslike low-temperature lattice vibrations have been convincingly established for $0.2 \leqslant x \leqslant 0.6$.[20,36] The thermal conductivity of the undoped mixed crystal $(KBr)_{0.5}(KCl)_{0.5}$ shows no phonon scattering below 1 K other than Casimir boundary scattering, and above $\sim$10 K the well-known scattering by a resonant mode.[37] By contrast, the CN^--doped $(KBr)_{0.5}(KCl)_{0.5}$ mixed crystals show phonon scattering leading to a thermal conductivity varying as T^2:

$$\Lambda_{0.2\%} = 13.0\times10^{-3}\ \mathrm{T}^2\ \mathrm{W\ cm^{-1}K^{-3}},$$

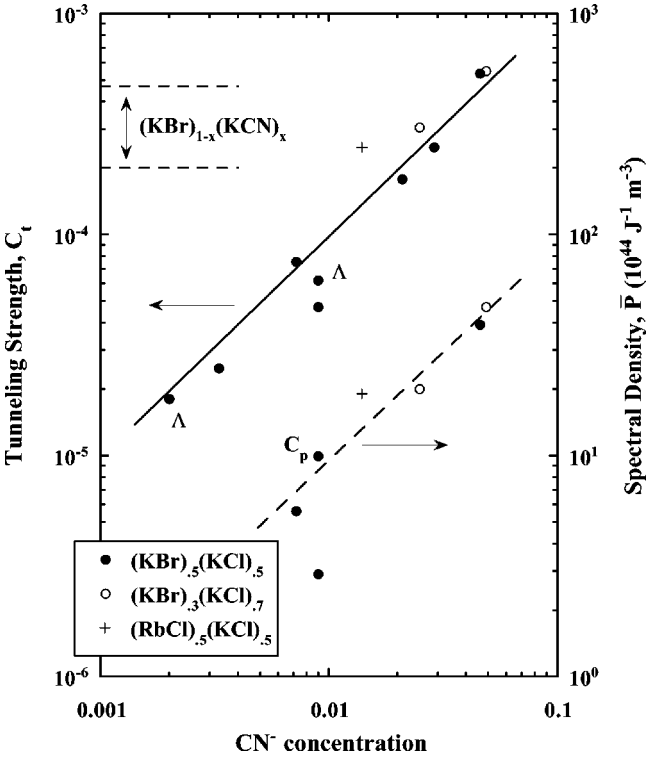

FIG. 13. Tunneling strength C_t (left axis) and $\bar{P}$ (right axis) primarily from internal friction measurements, for the three strained hosts (inset), as listed in Tables II and III. Two C_t values from thermal conductivity are labeled Λ, and one $\bar{P}$ value from specific heat is labeled C_p. Lines through each data set are guides to the eye of slope one. [The lowest data point for $\bar{P}$ is notably lower than the rest, for which we have no good explanation, other than to point out that it is derived from Watson's (Ref. 18) only internal friction measurement of these strained host crystals. Interestingly, her speed of sound data on the same crystal would give a value of $\bar{P}$ in much better agreement with the current work, see Table II.] The double arrow indicates the range of C_t obtained for mixed $(KBr)_{1-x}(KCN)_x$ crystals in which glasslike excitations have been observed (from Tables II and III). Note that only internal friction and thermal conductivity were considered for this range.

$$\Lambda_{0.9\%} = 3.8\times10^{-3}\ \mathrm{T}^2\ \mathrm{W\ cm^{-1}K^{-3}}, \qquad (5)$$

for the 0.2% and the 0.9% CN-doped crystal, respectively. Using the usual simplifying assumptions of averaging over speeds of sound, and over coupling energies (longitudinal and transverse) as explained in Refs. 34 and 20, the tunneling strengths C_t have been derived from Eq. (5), and are entered in Table III.

In Fig. 12, Watson's specific-heat data[30,18] have been redrawn in order to facilitate both the comparison of the doped versus the undoped strained crystal data, and also the extraction of the linear specific-heat term observed in the doped sample. Figure 12(a) shows the specific heat divided by the temperature cubed, below 50 K. Pure KBr at the lowest temperature, 1.7 K, approaches the Debye regime and agrees well with lower-temperature measurements,[20] indicated as the long-dashed line. The measurements on the undoped mixed crystal (circles) are very similar; C_p/T^3 is almost independent of temperature below 2 K, and the rise at the

TABLE II. Tunneling model parameters for the CN^--doped alkali-halide mixed host crystals. Elastic measurements from this work, except as indicated: Parameters from Q^{-1} data are given first, those from $\Delta v/v$ data are reported in parentheses. Also shown is the coupling energy γ_t of CN in KCl in the dilute limit from Ref. 33. Values for $(KBr)_{1-x}(KCN)_x$ and a-SiO_2 are included for comparison.

Material	ρ (g/cm^3)	v_t, 1 K (km/s)	$(\bar{P}\gamma_t^2/\rho v_t^2)\times 10^4$	γ_t (eV)	$\bar{P}$ (10^{44} J^{-1} m^{-3})
$(KBr)_{.5}(KCl)_{.5}$ host					
. . . + 0.33% CN	2.43	1.46	0.25[a]	[a]	[a]
. . . + 0.72% CN	2.44	1.42	0.75;(1.0)	0.16;(0.14)	5.6;(9.3)
. . . + 0.9% CN[b]	2.42[c]	1.42[d]	0.47;(0.74)	0.18;(0.14)	2.9;(7.6)
. . . + 2.1% CN	2.42	1.43	1.8[a]	[a]	[a]
. . . + 2.9% CN	2.42	1.35	2.5[a]	[a]	[a]
. . . + 4.6% CN	2.41	1.31	5.4;(7.6)	0.15;(0.17)	39;(44)
$(KBr)_{.3}(KCl)_{.7}$ host					
. . . + 2.5% CN	2.25	1.46	3.1;(4.0)	0.17;(0.16)	20;(31)
. . . + 4.9% CN	2.25	1.36	5.5;(8.9)	0.14;(0.16)	47;(55)
$(RbCl)_{.5}(KCl)_{.5}$ host					
. . . + 1.4% CN	2.44	1.38	2.5;(3.2)	0.16;(0.16)	19;(22)
$(KBr)_{1-x}(KCN)_x$ mixed crystals					
. . . $x=0.19$[e,f]	2.59[g]	1.05[g]	[h](25)		
. . . $x=0.41$[e,f]	2.32[g]	1.0[g]	4.7(5.6)		
. . . $x=0.75$[i]			4.5[j]		
KCl:CN					
45 ppm	1.989	1.7	not available	0.192[k]	not available
Amorphous silica					
a-SiO_2 [l]	2.20	3.78	3.3;(3.3)	0.9;(1.1)	4.8;(3.4)

[a]Measurements were not taken at temperatures low enough to find $C_t=\bar{P}\gamma_t^2/\rho v_t^2$ from $\Delta v/v$, or γ_t from either measurement. The internal friction value for C_t is simply found from the plateau value, $Q_0^{-1}=(\pi/2)C_t$.

[b]Measurements from Ref. 18.

[c]Reference 30, p. 160, measured at 300 K.

[d]Extracted from elastic measurements, this work.

[e]Elastic measurements by Berret *et al.* (Ref. 36), on two samples with nominally $x=0.25$ and $x=0.50$. Tunneling model fits were performed by us, without the use of an additional parameter (μ) used in Ref. 36.

[f]Composition redetermined by Watson *et al.* (Ref. 48).

[g]Reference 48.

[h]Attenuation measured below 1 K only.

[i]Reference 49.

[j]K. Knorr supplied the absolute scale for this measurement.

[k]Determined from the data shown in Fig. 2(a) of Ref. 33.

[l]Reference 34.

lowest temperatures of measurement, below 0.2 K, is believed to be caused by the experimental addenda. Their effect (the solid line) has been estimated, and has also been compared through measurements on a high-purity KBr sample.[20] Note in Fig. 12(a) the addenda heat capacity has not been subtracted from the measured data. In the CN^--doped strained crystal, C_p/T^3 rises rapidly below 1 K, and at the lowest temperatures completely masks any effect the addenda might have.

In Fig. 12(b), C_p of the 0.9% CN^--doped strained crystal is plotted as C_p/T vs T^2 on linear scales. A best-fit line to the data (rms deviation 1.64×10^{-7}) reveals from the ordinate intercept the magnitude of c_1, the linear specific-heat anomaly, and the slope of the line gives the T^3 coefficient. The formula of the line is then

$$\frac{C_p}{T}=c_1+(c_3+c_D)T^2, \tag{6}$$

where we find

$$c_1=6.4\times 10^{-7}\ \text{J g}^{-1}\text{K}^{-2},$$

$$(c_3+c_D)=5.6\times 10^{-6}\ \text{J g}^{-1}\text{K}^{-4}.$$

The Debye term, c_D, taken from the average value of C_p/T^3 of the undoped sample around 2 K [see Fig. 12(a)] gives

$$c_D=5.4\times 10^{-6}\ \text{J g}^{-1}\text{K}^{-4},$$

making the c_3 value negligibly small, as also seen in fluorite crystals by Cahill.[38] (Note that our best-fit coefficients are slightly different from those reported by Watson in Ref. 18.)

Using the tunneling model, $\bar{P}$ can be extracted from the value of c_1. A linear temperature dependence of the specific heat indicates a constant, energy-independent density of states $n(E)$, and for two-level systems[39]

TABLE III. Tunneling model parameters for the CN^--doped alkali-halide mixed host crystals calculated from thermal measurements. Values for $(KBr)_{1-x}$ $(KCN)_x$ and a-SiO_2 are included for comparison.

Material	ρ (g/cm^3)	v_t,1 K (km/s)	$(\bar{P}\gamma_t^2/\rho v_t^2)\times 10^4$	γ_t (eV)	$\bar{P}$ (10^{44} J^{-1} m^{-3})
$(KBr)_{0.5}(KCl)_{0.5}$ host					
. . . +0.2% CN[a]	2.43	1.46	0.18[b]		
. . . +0.9% CN	2.42[c]	1.42	0.62[b]		9.9[d]
$(KBr)_{1-x}(KCN)_x$[e]					
. . . $x=0.19$	2.59[f]	1.05[f]	2.6[g]		
. . . $x=0.41$	2.32[f]	1.0[f]	2.0[g]		
. . . $x=0.60$	2.09[f]	1.03[f]	4.2[g]		
Amorphous silica					
a-SiO_2	2.20	3.78	3.0[h]		1.0[i]

[a]Same crystal boule as for 0.33% elastic measurements.
[b]Thermal conductivity data from Ref. 18. Tunneling strength C_t is calculated according to Eq. (8) of Ref. 35.
[c]Reference 30.
[d]Heat-capacity data from Ref. 30. The value of $\bar{P}$ is our calculation [Eq. (9)] from the low-temperature linear specific-heat value, $c_1=6.4\times10^{-7}$ J g^{-1} K^{-2}. As stated in the text, the uncertainty of the logarithmic term in Eq. (8) also affects this value.
[e]Composition redetermined by Watson *et al.* (Ref. 48).
[f]Reference 48.
[g]Thermal-conductivity measurements (Ref. 20).
[h]Thermal-conductivity measurements (Ref. 50).
[i]Approximate value ($\pm$20%), based on a critical review of many investigations (Refs. 51 and 52). Note, however, a fundamental problem caused by a suspected minimum tunnel splitting.

$$c_1=\frac{\pi^2 k_B^2}{6\rho}n(E), \tag{7}$$

where k_B is Boltzmann's constant, and ρ the mass density. $n(E)$, however, is dependent on the measuring time t, since during that time only states with relaxation times shorter than t will be observed. The connection between $n(E)$ and $\bar{P}$ and the measuring time is given by[6]

$$n(E)=\frac{\bar{P}}{2}\ln[4t/\tau_m(E)], \tag{8}$$

where $\tau_m(E)$ is the shortest relaxation time for states of energy E at the measuring temperature. Experimentally, during normal long-time thermal measurements, the logarithmic term has been found to range between 5 and 20, and is often taken as 10 (see Ref. 4), which we also will do here. Combining this with the experimental value of c_1 and Eqs. (7) and (8), we find

$$6.4\times10^{-7}\ \text{J g}^{-1}\ \text{K}^{-2}=\frac{\pi^2 k_B^2}{6\rho}\frac{\bar{P}}{2}10. \tag{9}$$

The value $\bar{P}=9.9\times10^{38}$ J^{-1} cm^{-3} determined from this is also listed in Table III (where ρ is also listed).

By inspection of Tables II and III, it is seen that both C_t and $\bar{P}$ increase with the CN^- doping. Figure 13 shows this graphically. Plotted on the abscissa is the mole fraction of CN^- in solid solution, on the left axis the tunneling strength C_t, and on the right axis, the spectral density $\bar{P}$ of the tunneling states. The unmarked symbols indicate values taken from the internal friction measurements. The values taken from the speed of sound have not been plotted, since it was decided that the small temperature range of measurement below the maximum (Fig. 10) made the analyses less reliable. However, even inclusion of these values would not change the plots significantly. The value taken from the thermal measurements are labeled "Λ" for thermal conductivity, and "C_p" for specific heat. The straight lines indicate linear proportionality, and it appears quite clear that both C_t and $\bar{P}$ vary proportionally to the CN^- concentration over the entire doping range studied. We will return to this important point in the next section.

Although our discussion will concentrate on the elastic and thermal data below 10 K, we want to mention briefly the relaxation peak observed in the CN^--doped $(KBr)_{0.3}(KCl)_{0.7}$ crystals at $\sim$40 K. It is a single Debye relaxation peak, and is described well with the parameters given in Fig. 14. It is remarkable that this peak appears to be entirely unaffected by the random stresses in the host. Since it does not scale with the CN^- concentration, as shown in Fig. 8, it is probably not connected with relaxation involving these ions.

V. DISCUSSION

The fits of the experimental data to the tunneling model described in the previous chapter also yield the coupling energy γ_t of the tunneling center. γ_t is, with remarkably little scatter, 0.16 eV, very close to the value determined from optical dichroism measured on the CN^- ion (0.15 eV).[13] This is taken as convincing evidence that the tunneling entities observed here are indeed CN^- ions. The same conclu-

sion has been reached previously during numerous investigations on CN^--doped alkali halides in small concentrations,[14] and also, perhaps somewhat less convincingly, on mixed alkali-halide cyanide crystals.[20]

In order to determine the number density of the tunneling CN^- ions, we turn to the specific-heat measurement. From Eq. (7), and the measured value of c_1, we find the density of states,

$$n(E) = 4.9 \times 10^{39} \ \mathrm{J}^{-1}\,\mathrm{cm}^{-3}. \tag{10}$$

The internal friction plateau extends to ~ 10 K. Hence, $\overline{P}$ and thus $n(E)$ are expected to remain constant up to that temperature. Thus, the maximum energy is $E = 10\ \mathrm{K}\, k_B$, and therefore n_{TS}, the number density of tunneling CN^- ions observed up to 10 K, is

$$n_{TS} = n(E) \times 10\ \mathrm{K}\, k_B = 6.8 \times 10^{17}\ \mathrm{cm}^{-3}, \tag{11}$$

for the sample containing 0.9% CN^- ions. The number density of halide ions in the host is 1.5×10^{22} cm^{-3} (Table I), and therefore, 0.9% equals a number density

$$n_{\mathrm{CN}} = 1.4 \times 10^{20}\ \mathrm{cm}^{-3}, \tag{12}$$

which is equal to

$$\approx 200 n_{TS}. \tag{13}$$

This means that in the strained host, less than 1% of the dissolved CN^- ions can tunnel below 10 K, while the majority is frozen in. Since we have found that $\overline{P}$ scales with CN^- concentration (see Fig. 13), and since $\overline{P}$ also scales with $n(E)$ [Eq. (8)], which in turn scales with n_{TS} [Eq. (11)], it follows that the fraction of tunneling ions is the same for all doping levels investigated. Thus, what determines whether the CN^- ions can tunnel is their immediate environment, i.e., the random local strains, and not the CN^- ions in their neighborhood. Pairs or larger clusters of CN^- ions do not show up in the strained crystals, because their influence would lead to nonlinearity.

The observations described here show that in these doped, strained crystals noninteracting tunneling states are formed with the spectral distribution as postulated in the tunneling model. Thus, crystals such as $(KBr)_{0.5}\,(KCl)_{0.5}$:CN can be viewed as experimental models for testing a theoretical model proposed for amorphous solids. Beyond that, these experiments also show clearly that random stresses alone, not interactions, can lead to glasslike excitations in a crystal. In this particular case, the role of the stresses is to spread the tunneling frequencies of the CN^- ions, while immobilizing their majority. Similarly, it appears reasonable to expect that random stresses will lead to tunneling in crystals in which such motion does not occur in the unstressed lattice. In $(BaF_2)_{1-x}(LaF_3)_x$, for example, the relaxation rate of the interstitials at small concentrations is consistent with a barrier height of ~ 0.5 eV,[40] which is in turn consistent with the observation that isolated defects do not contribute to low-temperature internal friction, i.e., they are frozen in. Yet, as the concentration increases, the internal friction approaches that characteristic of amorphous solids.[38,29] Another example is CN^- in the NaCl host lattice.[41] At concentrations of 2.5% and below, the tunnel splitting is so small that no phonon scattering is observed in low-temperature thermal-conductivity experiments, i.e., the potential barriers are high. Yet, at higher concentrations, the mixed crystals show lattice vibrations similar to those found in amorphous solids (e.g., a thermal conductivity varying as T^2). Yet another example are mixed alkali-cyanide crystals. Pure KCN (Ref. 20) and NaCN (Refs. 41 and 42) have low-temperature specific heats obeying the Debye law. The CN^- ions are frozen in, in an antiferroelectric phase. In the mixed crystal $(KCN)_{1-x}$ $(NaCN)_x$, however, the lattice vibrations are clearly glasslike, as shown by both thermal conductivity[20] and specific heat. Based on what we have seen in the present study, we suggest that in both NaCl:NaCN and NaCN:KCN random stresses are the most likely cause for the tunneling states. The natural extension of these observations is the idea that the variable spacing of the atoms or molecules in amorphous solids will also lead to tunneling states with a constant spectral distribution, $\overline{P}$. This is the assumption which forms the basis of the tunneling model.[2,3]

While this work explains the existence of tunneling states in amorphous solids, regardless of their chemical composition, it offers no clue about their universality, or more precisely, about the universality of their tunneling strengths, C. In fact, the data shown in Fig. 13 give no hint of a saturation with increasing CN^- concentration, although the tunneling strength appears to exceed those observed in the mixed crystal $(KBr)_{1-x}(KCN)_x$ in which glasslike excitations have been studied extensively.[20,36] The range of C measured on these crystals is listed in Tables II and III, and is also indicated on the left axis of Fig. 13. This may be taken as evidence that random stresses alone cannot lead to a saturation of the tunneling strength within the universal range, and that another mechanism is needed, e.g. interaction between the CN^- quadrupoles, as has been discussed by Sethna and Chow,[43] based on quadrupolar interactions first suggested by Klein *et al.*[10] For the saturation of the tunneling strength in

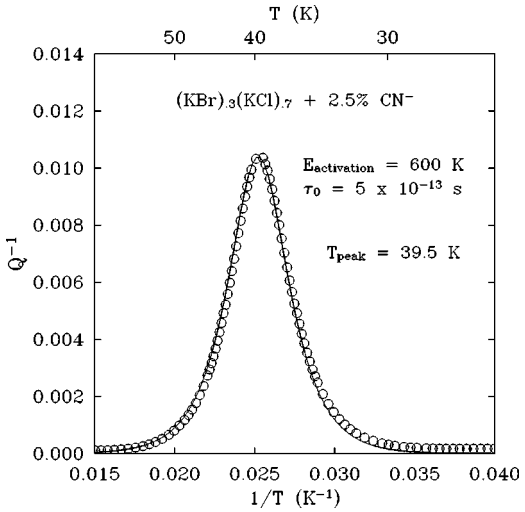

FIG. 14. Relaxation peak observed in $(KBr)_{0.3}(KCl)_{0.7}+2.5\%$ CN^-. The solid curve is a fit to a Debye relaxation, with the parameters as shown in the figure.

ion-implanted silicon,[44] an alternative explanation has been suggested: As the random stresses build, the yield stress is finally locally exceeded. This will lead to a rearrangement of the atoms, which will limit the formation of more tunneling states. In pursuing this picture, we note that in our mixed crystals the random stresses are dominated by the host atoms which, however, have not exceeded the yield stress. Therefore, the tunneling strength and spectral density increase in linear proportion with the CN^- doping. Saturation will require larger random stresses as produced, for instance, by increasing the CN^- concentration in excess of those we have been able to prepare. In the mixed crystals such as $(BaF_2)_{1-x}(LaF_3)_x$, which we reviewed above, this yield stress may have been exceeded for large x, leading to a saturation of the tunneling strength.

In conclusion, doped mixed crystals have been used successfully to create tunneling states with the same spectral distribution as observed in amorphous solids, thus supporting the picture that random stresses, or the variation of interatomic spacings, are the cause for these states. Whether they also cause the universality of the tunneling strength remains a tempting, yet so far unanswered, question.

ACKNOWLEDGMENTS

Many discussions about this work with Drs. Susan Watson and David Cahill, are gratefully acknowledged. This work was supported by the Cornell Center for Materials Research, Award No. DMR-9121564. Special thanks are due to Gerhard Schmidt for sample preparation and Drs. John Hunt and E. Lobkowsky for x-ray measurements. We thank Dr. F. Lüti (University of Utah) for help with determining the CN^- concentration. The financial support by the National Science Foundation, Grant No. DMR-9115981, is also gratefully acknowledged.

*Present address: Department of Physics and Astronomy, Bowdoin College, Brunswick, Maine 04011.

†FAX: (607) 255-6428. Email address: pohl@ccmr.cornell.edu

[1] Reviewed in *Amorphous Solids: Low Temperature Properties*, edited by W. A. Phillips (Springer Verlag, New York, 1981).

[2] P. W. Anderson, B. I. Halperin, and C. M. Verma, Philos. Mag. **25**, 1 (1972).

[3] W. A. Phillips, J. Low Temp. Phys. **7**, 351 (1972).

[4] J. F. Berret and M. Meissner, Z. Phys. B: Condens. Matter **70**, 65 (1988).

[5] J. Jaeckle, Z. Phys. **257**, 212 (1972).

[6] S. Hunklinger and A. K. Raychaudhuri, in *Progress in Low Temperature Physics*, edited by D. F. Brewer (Elsevier, New York, 1986), p. 265, Vol. IX.

[7] W. A. Phillips, Rep. Prog. Phys. **50**, 1657 (1987).

[8] *Tunneling Systems in Amorphous and Crystalline Solids*, edited by P. Esquinazi (Springer, Berlin, 1998).

[9] R. O. Pohl, Xiao Liu, and E. Thompson, Rev. Mod. Phys. (to be published).

[10] M. W. Klein, B. Fischer, A. C. Anderson, and P. J. Anthony, Phys. Rev. B **18**, 5887 (1978).

[11] D. A. Parshin, Phys. Solid State **36**, 991 (1994).

[12] F. Lüty, Phys. Rev. B **10**, 3677 (1974).

[13] H. U. Beyeler, Phys. Rev. B **11**, 3078 (1975).

[14] V. Narayanamurti and R. O. Pohl, Rev. Mod. Phys. **42**, 201 (1972).

[15] C. Enss, H. Schwoerer, D. Arndt, M. V. Schickfus, and G. Weiss, Europhys. Lett. **26**, 289 (1994).

[16] M. C. Foote and B. Golding, Phys. Rev. B **43**, 9206 (1991).

[17] R. O. Pohl and M. Meissner, Phys. Rev. Lett. **67**, 1469 (1991).

[18] S. K. Watson, Phys. Rev. Lett. **75**, 1965 (1995).

[19] C. Enss, R. Weis, S. Ludwig, and S. Hunklinger, Czech. J. Phys. **46**, 3287 (1996).

[20] J. J. De Yoreo, W. Knaak, M. Meissner, and R. O. Pohl, Phys. Rev. B **34**, 8828 (1986).

[21] F. Lüty, in *Defects in Insulating Crystals*, edited by V. M. Turchkevich and K. K. Shvarts (Springer-Verlag, Berlin, 1981), p. 69.

[22] W. D. Seward and V. Narayanamurti, Phys. Rev. **148**, 463 (1966).

[23] L. Vegard, Z. Phys. **5**, 17 (1921).

[24] D. G. Cahill and J. E. Van Cleve, Rev. Sci. Instrum. **60**, 2706 (1989).

[25] Karen A. Topp, Ph.D. thesis, Cornell University, 1997.

[26] E. T. Swartz, Rev. Sci. Instrum. **57**, 2848 (1986).

[27] X. Liu, E. Thompson, B. E. White, Jr., and R. O. Pohl, Phys. Rev. B **59**, 11 767 (1999).

[28] E. Thompson, Ph.D. thesis, Cornell University, 2000.

[29] K. A. Topp, E. J. Thompson, and R. O. Pohl, Phys. Rev. B **60**, 898 (1999).

[30] Susan K. Watson, Ph.D. thesis, Cornell University, 1992.

[31] R. Feile, A. Loidl, and K. Knorr, Phys. Rev. B **26**, 6875 (1982).

[32] N. E. Byer and H. S. Sack, Phys. Status Solidi **30**, 569 (1968).

[33] P. Nalbach, O. Terzidis, K. A. Topp, and A. Würger, J. Phys.: Condens. Matter **13**, 1467 (2001).

[34] J. E. Van Cleve, A. K. Raychaudhuri, and R. O. Pohl, Z. Phys. B: Condens. Matter **93**, 479 (1994).

[35] K. A. Topp and D. G. Cahill, Z. Phys. B: Condens. Matter **101**, 235 (1996).

[36] J. F. Berret, P. Doussineau, A. Levelut, M. Meissner, and W. Schön, Phys. Rev. Lett. **55**, 2013 (1985).

[37] R. O. Pohl, in *Localized Excitations in Thermal Conductivity*, edited by R. F. Wallis (Plenum, New York, 1968), p. 434.

[38] D. G. Cahill and R. O. Pohl, Phys. Rev. B **39**, 10 477 (1989).

[39] R. B. Stephens, Phys. Rev. B **8**, 2896 (1973).

[40] *Crystals with the Fluorite Structure*, edited by W. Hayes (Clarendon, Oxford, 1974).

[41] S. K. Watson and R. O. Pohl, Phys. Rev. B **51**, 8086 (1995).

[42] B. Mertz, J. F. Berret, R. Böhmer, A. Loidl, M. Meissner, and W. Knaak, Phys. Rev. B **42**, 7596 (1990).

[43] J. P. Sethna and K. S. Chow, Phase Transitions **5**, 315 (1985).

[44] Xiao Liu, P. D. Vu, R. O. Pohl, F. Schiettekatte, and S. Roorda, Phys. Rev. Lett. **81**, 3171 (1998).

[45] *Numerical Data and Functional Relationships in Science and Technology*, edited by K.-H. Hellwege, Landolt-Börnstein New Series, Group III, Vol. 7, Pt. a (Springer-Verlag, New York, 1973).

[46] *CRC Handbook of Chemistry and Physics*, 67th ed., edited by R. C. Weast (CRC Press, Boca Raton, 1986), p. F-157.

[47] A. Loidl, R. Feile, and K. Knorr, Z. Phys. B: Condens. Matter **42**, 143 (1981).
[48] S. K. Watson, D. G. Cahill, and R. O. Pohl, Phys. Rev. B **40**, 6381 (1989).
[49] K. Knorr, U. G. Volkmann, and A. Loidl, Phys. Rev. Lett. **57**, 2544 (1989).
[50] A. K. Raychaudhuri and R. O. Pohl, Solid State Commun. **44**, 711 (1982).
[51] M. Meissner (private communication).
[52] P. Strehlow and M. Meissner, Physica B **263**, 273 (1999).
[53] D. G. Cahill, S. K. Watson, and R. O. Pohl, Phys. Rev. B **46**, 6131 (1992).
[54] F. C. Baumann, J. P. Harrison, R. O. Pohl, and W. D. Seward, Phys. Rev. **159**, 691 (1967).